Available online at www.sciencedirect.com
ScienceDirect
Acta Biomaterialia 2 (2006) 537–546
Acta BIOMATERIALIA
www.actamat-journals.com

Analytical model for residual stresses in polymeric containers during cryogenic storage of hematopoietic stem cells

David M. Saylor [a,*], Martin K. McDermott [a], Edwin R. Fuller Jr. [b]

[a] *Food and Drug Administration, Center for Devices and Radiological Health, Office of Science and Engineering Laboratories, Rockville, MD 20852, United States*

[b] *National Institute of Standards and Technology, Materials Science and Engineering Laboratories, Ceramics Division, Gaithersburg, MD 20899, United States*

Received 13 February 2006; received in revised form 26 April 2006; accepted 11 May 2006

Abstract

Hematopoietic stem cell (HSC) therapy can significantly lower instances of infection in chemotherapy patients by accelerating the recovery of white blood cells in the body. However, therapy requires that HSCs be stored at cryogenic temperatures to retain the cells' ability to proliferate. Currently, cells are stored in polymeric blood bags that are subject to fracture at the extremely low storage temperatures, which leads to cell contamination, thereby reducing their effectiveness. Therefore, we have developed an analytical model to predict the accumulation of stresses that ultimately lead to crack initiation and bag fracture during cryogenic storage. Our model gives explicit relationships between stress state in the container and thermoelastic properties of the container material, container geometry, and environmental factors that include temperature of the system and pressure induced by excess gas evolving from the stored medium. Predictions based on the model are consistent with experimental observations of bag failures that occurred during cryogenic storage applications. Finally, the model can provide guidance in material selection and bag design to fabricate bags that will be less susceptible to fracture.

Keywords: Blood bags; Hematopoietic stem cells (HSC); Cryogenic storage; Failure model; Residual stresses; Thermal expansion mismatch; Gas evolution

1. Introduction

During chemotherapy, the number of white blood cells in the patient's body is dramatically reduced, which can lead to infection and even death. However, hematopoietic stem cell (HSC) therapy can significantly lower these adverse instances by promoting the recovery of a patient's white blood cell count [1]. During HSC therapy, the stem cells are extracted from the patient prior to the chemotherapy treatment and stored until after the treatment is completed. The cells are then reintroduced into the patient, and about a month later, the patient's white blood cell count returns to normal, significantly reducing the risk of infection.

One of the major problems with HSC therapy is the contamination of the cells, which can limit their effectiveness. Cell contamination occurs primarily during the storage phase of the therapy due to failure of the storage container. Currently, HSCs are stored in blood bags that have been developed, tested, and cleared by the FDA for use in storing cells with no nuclei such as red blood cells and platelets at 193 K [2]. However, previous studies have shown that nucleated cells such as HSCs have less ability to proliferate after thawing if stored above 113 K [3]. Therefore, hospitals began using blood bags to store HSCs at liquid nitrogen temperatures (~77 K), significantly below the approved storage temperature of the bags. The practice

* Corresponding author. Tel.: +1 301 827 4717.
E-mail address: david.saylor@fda.hhs.gov (D.M. Saylor).

1742-7061/$ - see front matter
doi:10.1016/j.actbio.2006.05.006

of using blood bags for HSC storage at these extremely low temperatures has resulted in numerous reports of blood bag fracture, resulting in contamination of the contents [4,5]. Depending on the bag material, failure rates of up to about 10% have been reported [5]. Of these failures, 42% ultimately resulted in cell contamination.

Blood bag failure at liquid nitrogen temperatures is typically characterized by brittle fracture [6,7]. At temperatures below the glass transition temperature (T_g), polymeric materials are stiff and have little ability to dissipate applied strain through viscous relaxation [4,8,9]. Thus, the application of strain to the polymer can result in a considerable accumulation of stress in the material. Stress gives rise to elastic strain energy that provides the driving force for the nucleation and propagation of cracks that lead to failure of the blood bag. Further, the magnitude of the accumulated stresses is sensitive to the geometry of the blood bag. Therefore, to formulate a predictive model for the failure of blood bags during the cryogenic storage of stem cells, it is critical to elucidate the origins of these stresses and to quantify the influence of bag material and geometry on the accumulated stresses and, thereby, fracture.

Two potential strain mechanisms that can give rise to residual stresses in these systems have been identified and are illustrated in Fig. 1. The first originates due to a thermal expansion mismatch between the frozen stem cell medium and its polymeric container. The thermal expansion coefficients of polymeric materials at cryogenic temperatures typically range from 3×10^{-5} to $8\times10^{-5}\,K^{-1}$ [9–11]. The frozen cell medium, however, will, on average, have a lower thermal expansion coefficient of approximately $2.5\times10^{-5}\,K^{-1}$ over the same temperature range, assuming the medium's behavior is analogous to that of ice [12]. Therefore, as the system is cooled, the blood bag will contract at a faster rate than the medium. Because the medium is elastically stiff, it does not yield to this contraction and significant residual stresses can accumulate in the blood bag. This is shown schematically in Fig. 1a.

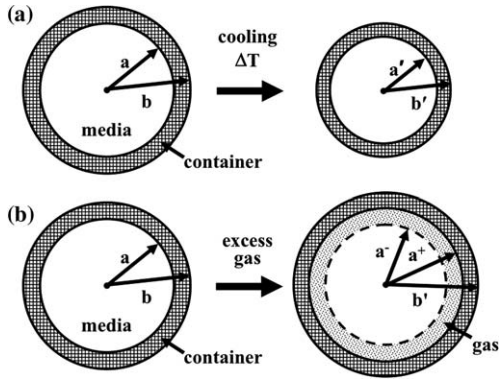

Fig. 1. Schematic representation of two potential mechanisms that can induce strain, and thereby residual stresses, in the polymeric container. These mechanisms are: (a) a temperature change when there is a thermal expansion mismatch between the container and medium and (b) excess gas evolving from the medium.

The second potential mechanism of residual stress generation derives from the presence of gases in the medium (private communication, Cullis HM, American Fluoroseal). The premise is that as the medium solidifies, dissolved gases, such as CO_2, segregate out of solution and form gas bubbles, which are trapped in the frozen medium. As the system is cooled to 77 K, these gases will solidify and leave evacuated voids within the frozen medium. During storage at 77 K, nitrogen diffuses through the polymer and the frozen medium into these voids. As the system is thawed, the condensed gases will return to a gaseous state, so the voids will contain the original amount of gas plus the nitrogen that migrated in during storage. The increased pressure within the voids will drive the nitrogen out of the frozen medium, and the "evolved" gas will build up a gas layer between the medium and the polymeric blood bag (see Fig. 1b), which is still brittle (i.e., below the glass transition temperature). This phenomenon will result in an increased pressure against the wall of the blood bag that gives rise to residual stresses.

It is not clear how these two mechanisms (contraction during freezing and gas expansion during thawing), individually or in combination, contribute to the overall stress state in blood bags during the cryogenic storage of stem cells. Therefore, it is the goal of this work to derive an analytical model for the stress state that evolves in blood bags based on these two mechanisms. The model will allow us to determine the relative effects of each mechanism and their variation with the type of blood bag material and geometric design.

In this paper, we describe the derivation and application of an analytical model for the stress state of blood bags filled with HSCs at cryogenic temperatures based on contributions from thermal expansion mismatch and evolved gases. In the next section, we give a detailed outline of the model and its derivation. The subsequent section describes results of the application of the model to elucidate the effects of strain mechanism, material, and bag geometry on the stress state. This is followed by a discussion of the results, and finally, a brief summary.

2. Materials and methods

2.1. Overview

The objective of this work was to develop an analytical model of the stress state in polymeric blood bags that arises due to strains induced from thermal expansion mismatch during freezing and/or excess gas evolution during thawing. During freezing and thawing of blood bags containing cell medium, the largest stresses, and therefore strain energies, accumulate at temperatures below the T_g of the polymer. At these temperatures, viscous stress relaxation mechanisms in the polymer are negligible. Further, above their T_g the polymer materials (elastomers) that comprise the bags are elastically soft and can accommodate very large strains (~300%) before yielding. Therefore, although

there may be a significant amount of strain induced in the bag, no substantive amount of elastic strain energy or permanent deformation will accrue above T_g due to the extremely low stiffness and large strain to failure of these materials. Thus, we assume that elastic strain energy accumulated in the polymer above T_g is negligible and that the mechanical response of both the blood bag and medium below T_g can be approximated by linear elasticity theory. Note that the T_g values for elastomeric materials that comprise the bags (<230 K) are significantly less than the freezing temperature of the medium (~269 K), thus only the influence of the frozen medium on the accumulation of residual stresses is considered.

To continue with the derivation of the model, we further assume that both the blood bag and medium have isotropic thermoelastic properties that are independent of temperature. This should be a reasonable approximation because we expect the extent of the variation in thermoelastic properties in each component over the temperature ranges of interest (i.e., below T_g of the polymer) to be less than a factor of two. We note that the properties of both the polymer and the frozen medium will contain microscopic variations, which will result in a stress state that varies on a microscopic level. By ignoring these variations, the stress states determined by our model must be considered an averaged, bulk material response.

Next, we use a simplified system geometry that consists of two concentric spheres that represent the biological medium contained inside a polymeric blood bag shell. This geometry is illustrated in Fig. 1a. Although the model geometry is only an approximation, it incorporates the geometric components of the bag that will have the largest impact on the stress state, the radius of curvature and the thickness of the bag. The concentric sphere geometry yields a relatively simple stress state as a function of position within the system. In fact, once the apparent pressure on the blood bag is determined, the stress state is completely specified.

Finally, to derive an expression for the apparent pressure, we start by considering the two mechanisms by which strain can be introduced into the system: thermal expansion mismatch and pressure due to evolved gases. Based on these considerations, functional forms for the displacements induced by these mechanisms can be specified for each region. We then introduce the boundary condition that the volume of gas between the blood bag and the medium must behave ideally. With this boundary condition, we can determine the apparent pressure on the blood bag, and the stress state of the system is completely specified.

2.2. Derivation

To derive a model for the state of stress that arises in the blood bag and the cell medium, we start with the general form for stress within a spherical shell (see Fig. 1 and Appendix A). Due to spherical symmetry, there are only two independent stress components at any position within the system. These are the radial component, σ^r, and the tangential component, $\sigma^\theta = \sigma^\phi$ (see Eq. (A.5) for the stresses in the medium and Eq. (A.7) for the stresses in the blood bag). Assuming that the radius of the medium, a, is large relative to the blood bag thickness, $t = b - a$, we set $R = b \approx a$, so the stress state in the blood bag is approximated by Eq. (A.9). These expressions, which include the misfit strains on cooling, give the stresses for the first mechanism, i.e., thermal expansion mismatch (Fig. 1a). The second mechanism requires consideration of the excess gas. Because the pressure (stress) in a newly formed intermediate gas region must be hydrostatic, and because continuity is required across the interfaces, the stress at the interface between the medium and the gas σ_{a^-} must equal the stress between the gas and the blood bag σ_{a^+}. Thus, we introduce $P = -\sigma_a = -\sigma_{a^-} = -\sigma_{a^+}$, where P is the gas pressure or the apparent pressure on the blood bag. With this, the stress state for the second mechanism after gas is evolved in the system can be expressed as follows. In the medium, the stress is hydrostatic and independent of radial position, r, thus

$$\sigma_1^r = \sigma_1^\theta = \sigma_1^\phi = -P. \tag{1}$$

In the bag material, the radial component of the stress is a function of radial position given by

$$\sigma_2^r(r) = -\left(\frac{R-r}{t}\right)P, \tag{2}$$

and the tangential component is a constant given by

$$\sigma_2^\theta = \sigma_2^\phi = \left(\frac{R}{2t}\right)P. \tag{3}$$

The derivation of Eqs. (1)–(3) is given in Appendix A. Upon examination of Eqs. (1)–(3), it is apparent that the only unknown is P. Thus, once P is determined, the stress at any position in the system is completely specified. Note that stresses of interest are those that arise in the blood bag. Since $R \gg t$, the tangential stress components within the bag are much greater than the internal pressure. In contrast, the radial stress component has a linear gradient across the bag thickness, going from the internal pressure P at the inner surface to atmospheric pressure (≈0) at the outer surface.

To determine P for the first mechanism, we must set a boundary condition based on the compatibility of displacements between the blood bag and the medium after deformation. Thus, we need first to specify a functional form for the displacements in the model. Due to the spherical symmetry of the model, the displacements are radial everywhere. Assuming that the medium and polymer are both elastically isotropic, the displacements in the medium, U_1, as a function of radial position can be expressed as (see Appendix A)

$$U_1(r) = \left[-\frac{P(1-2\nu_1)}{E_1} + \alpha_1 \Delta T\right] r, \tag{4}$$

where E_1, v_1, and α_1 are Young's modulus, Poisson's ratio, and the coefficient of thermal expansion, respectively, of the medium. Under the assumption that $R \gg t$, the radial displacements, U_2, in the blood bag are constant and given by (see Appendix A)

$$U_2(R) = U_2 = \frac{P(1-v_2)R^2}{2tE_2} + \alpha_2 \Delta T R, \tag{5}$$

where the subscripted dependent variables are the thermoelastic properties of the bag material. The first term in the equations is the displacement due to the pressure applied to the blood bag by the other components, the sought unknown, and the second term is the thermally induced displacement.

The next step in the derivation is to apply a compatibility condition on the displacements to obtain an expression for P. If there were no gas involved, one would simply set the displacement expressions at the interface radius equal to each other, $U_1(R) = U_2(R)$, and solve for P [13]:

$$P = 2\beta^{-1}\left(\frac{t}{R}\right)\left(\frac{E}{1-v}\right)\Delta\alpha(-\Delta T), \tag{6}$$

where $E = E_2$, $v = v_2$, i.e., the elastic properties of the blood bag material, $\Delta\alpha = (\alpha_2 - \alpha_1)$ and

$$\beta = 1 + \frac{(1-2v_1)E_2}{(1-v_2)E_1}\left(\frac{2t}{R}\right). \tag{7}$$

We note that the quantity $[2(1-2v_1)E_2]/[(1-v_2)E_1]$ is typically less than one and $t \ll R$, so $\beta \approx 1$. Since the temperature change is negative, i.e., $(-\Delta T) > 0$, and the thermal expansion mismatch $\Delta\alpha$ is positive, i.e., the blood bag contracts more than the medium, the interface pressure P is positive.

For the second mechanism, the evolution of excess gas in the system, the situation is more complex due to the gas physically separating the blood bag from the medium, thus destroying the displacement compatibility at the interface. Instead, we assume that the displacements are constrained such that the volume of gas, V, behaves ideally. This yields the equalities

$$V = \frac{nR_G T}{P} = \frac{4\pi}{3}\left(a_+^3 - a_-^3\right), \tag{8}$$

where n is the number of moles of gas, R_G, is the universal gas constant, and T is the absolute temperature of the system. Now, by setting $a_+ = R + U_2(R)$ and $a_- = R + U_1(R)$ and assuming the radial displacements are small relative to R, we can rewrite Eq. (8) as a quadratic equation in P,

$$\beta\frac{(1-v)R}{2tE}P^2 + \Delta\alpha\Delta T P - \frac{nR_G T}{4\pi R^3} = 0. \tag{9}$$

Solving Eq. (9) for P yields

$$P = P_1 \pm \sqrt{P_1^2 + P_2^2}, \tag{10}$$

where

$$P_1 = \beta^{-1}\left(\frac{t}{R}\right)\left(\frac{E}{1-v}\right)\Delta\alpha(-\Delta T), \tag{11a}$$

and

$$P_2 = \sqrt{2\beta^{-1}\left(\frac{t}{R}\right)\left(\frac{E}{1-v}\right)\left(\frac{nR_G T}{4\pi R^3}\right)}, \tag{11b}$$

We note that P_1 is one half the interface pressure defined by Eq. (6) for first mechanism. If there is no gas layer (i.e., $n = 0$), then $P_2 = 0$ and we recover Eq. (6), if we choose the + sign of the ± in Eq. (10). Similarly, if a gas layer is present with no temperature change (i.e., $P_1 = 0$), again the appropriate choice is the + sign in Eq. (10), since P must be positive, and in this case equal to P_2. So, in general the + sign in Eq. (10) is the appropriate choice.

Eq. (10) gives the explicit relationship between hydrostatic pressure exerted on the polymeric blood bag and its thermoelastic properties and geometry, as well as the amount of gas released from the medium and the amount of thermally induced strain. Eq. (10) can be substituted back into Eqs. (1)–(3), and therefore, the complete state of stress in the blood bag and medium is specified. In the next section, we utilize these equations to explore the effects of the various parameters on the stresses accumulated in the blood bag. Note that the equations derived here are not restricted to storage of stem cells and should be applicable to estimate the stress state in blood bags or any type of storage container regardless of the medium.

3. Results

In this section, we explore the effect of strain mechanism, material, and blood bag geometry on the stresses that arise in polymeric blood bags during stem cell storage at cryogenic temperatures. To determine these effects, we use a hypothetical material as a baseline that has the thermoelastic properties of a typical polymer at cryogenic temperatures. The hypothetical material was assumed to have the following thermal–elastic properties: $E = 10$ GPa, $v = 0.33$, $\Delta\alpha = 3 \times 10^{-5}\ \mathrm{K}^{-1}$ (in relation to the frozen medium), and $T_g = 218$ K. As stated in the previous section, we assume that any stress accumulated in the blood bag at temperatures above T_g is negligible, i.e., T_g is the stress-free temperature. In addition, we assume a baseline for the blood bag geometry, which is characterized by $R = 2 \times 10^{-2}$ m (approximately the average radius of a 50 ml blood bag) and $t = 2 \times 10^{-4}$ m, and therefore, $R/t = 100$. Finally, for most media the elastic properties are such that $\beta \approx 1$. Unless otherwise stated, these values are used in the calculations described in the following sections.

During the storage procedure (i.e., freezing and subsequent thawing of the system), Eq. (10) (with Eqs. (2) and (3)) demonstrates that the stress in the blood bag will be maximum at one of two positions along this temperature profile. The first is at the minimum temperature of 77 K

(liquid N_2) where the temperature difference relative to the stress-free temperature ($-\Delta T$), is a maximum. Further, at 77 K there should be no excess gas, and therefore, the stresses in the blood bag are only due to the thermal expansion mismatch. Assuming all of the gas present in the medium prior to freezing is carbon dioxide (CO_2), the second maximum in stress will occur at 177 K or the temperature where the solidified gas components of the medium return to a gaseous form. In the following sections we look at both of these possibilities and how they relate to the accumulation of stresses in blood bags.

3.1. Strain mechanism

One of the outstanding questions regarding the failure of blood bags at cryogenic temperatures is which of the two strain mechanisms, thermal expansion mismatch or evolved gases, is responsible for blood bag fracture? In other words, do they typically fail during the initial cooling stage or upon thawing? To answer this question, we start by considering the variation of the apparent pressure as a function of the temperature and number of moles of excess gas, $P(T,n)$. Now, we can represent the pressure at the two potential critical temperatures as $P(T^{\mathrm{L}},0)$ and $P(T^{\mathrm{H}},n)$, which are the pressure at lowest temperature to which the blood bag is exposed, T^{L}, in the absence of gas and the pressure at the temperature where n moles of previously solidified gas returns to a gaseous state, T^{H}, respectively. Setting these two pressures equal to each other and solving for n yields

$$n = \left(\frac{8\pi R^3}{R_{\mathrm{G}} T^{\mathrm{H}}}\right)\beta^{-1}\left(\frac{t}{R}\right)\left(\frac{E}{1-v}\right)(\Delta\alpha)^2(T^0 - T^{\mathrm{L}})(T^{\mathrm{H}} - T^{\mathrm{L}}), \tag{12}$$

where T^0 is the stress-free temperature when no gas is present. Therefore, Eq. (12) gives the number of moles of excess gas at T^{H} required to induce the same apparent pressure in the blood bag that would be observed at T^{L} when no gas is present. Taking $T^{\mathrm{L}} = 77$ K, $T^{\mathrm{H}} = 177$ K, and $T^0 = T_{\mathrm{g}} = 218$ K, the relationship between n and $\Delta\alpha$ is shown graphically in Fig. 2. Assuming the stresses that accumulate in the blood bag are sufficient to induce fracture, we expect that the blood bag should fail upon thawing when the excess gas is released for values of n and $\Delta\alpha$ above the plotted line. Conversely, for values below the line, the blood bag should fracture when cooled to the temperature of liquid nitrogen. Note that for the value of $\Delta\alpha$ corresponding to our hypothetical material ($\sim 3\times10^{-5}$ K^{-1}), at least 2×10^{-4} mol of excess gas is required for the evolution of gas from the medium to be the critical mechanism for bag failure.

3.2. Thermoelastic properties

In addition to evaluating the critical failure mechanism, the analytical model derived above can also be used to determine the effect of the thermoelastic properties (E, v, and $\Delta\alpha$) of the blood bag material on the stress that accumulates under different environmental conditions. This can be valuable in guiding a material selection process for a specific storage application. As mentioned above, the largest stresses in the blood bag will be tensile and tangential to the blood bag shell, and therefore, the tangential stress σ^{θ} is the stress component that will first exceed the fracture strength of the material resulting in fracture of the container. Thus, in this section, we evaluate the effect of the thermoelastic properties of the blood bag material on σ^{θ}. By combining Eqs. (10), (11) with Eq. (3), we find

$$\sigma^{\theta} = \frac{1}{2}\beta^{-1}\left(\frac{E}{1-v}\right)\left[(\Delta\alpha)(T^0 - T) + \sqrt{(\Delta\alpha)^2(T^0-T)^2 + \beta\left(\frac{R}{t}\right)\left(\frac{1-v}{E}\right)\left(\frac{nR_{\mathrm{G}}T}{2\pi R^3}\right)}\right], \tag{13}$$

We start by considering the effect of Poisson's ratio, v, on σ^{θ}. We note from Eq. (13) that v only appears in combination with the Young's modulus E as $E/(1-v)$. Furthermore, v typically varies only between 0.2 and 0.4 for most polymeric systems, so the maximum variation of $E/(1-v)$ with v is only 33% over the entire range of expected v values. Thus, we include the influence of Poisson's ratio with that of Young's modulus.

Fig. 3a shows the influence of the tangential stress $\sigma^{\theta}(E,\Delta\alpha)$ on Young's modulus E and thermal expansion mismatch $\Delta\alpha$ at 77 K in the absence of excess gas. With no excess gas, we see from Eq. (13) that σ^{θ} is directly proportional to both E and $\Delta\alpha$, which is also evident in the figure. Fig. 3a also illustrates that for a large ΔT, both of these relationships are quite strong, with variations in σ^{θ}

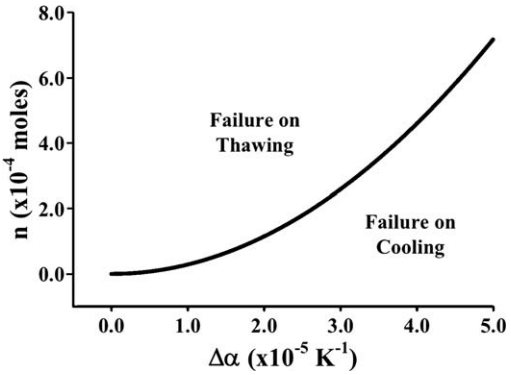

Fig. 2. Comparison of the mechanisms that can induce stress in the blood bag, thermal expansion mismatch ($\Delta\alpha$) and release of excess gas from the medium (n), assuming the maximum stress occurs at 77 K in the absence of excess gas and 177 K when excess gas is present. The plot shows the amount of excess gas, n, required at 177 K to yield an apparent pressure on the container, P, that is equivalent to the P induced from $\Delta\alpha$ at 77 K. Values shown assume that the system is stress-free at the polymer T_{g} in the absence of gas. The calculations were based on a container with dimensions $R = 2\times10^{-2}$ m and $t = 2\times10^{-4}$ m comprised of a hypothetical material with $E = 10$ GPa, $v = 0.33$, and $T_{\mathrm{g}} = 218$ K. Further, the media were assumed to have thermoelastic properties such that $\beta = 1$.

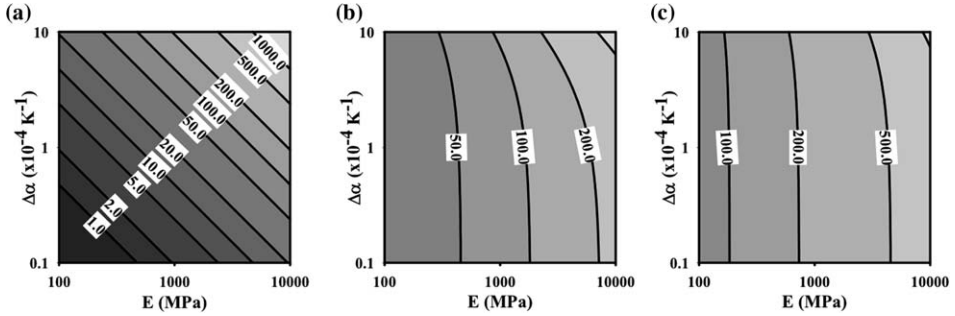

Fig. 3. Relationships between the tangential stress, σ^{θ}, on the container and the thermal–elastic properties of the container material, $\sigma^{\theta}(E,\Delta\alpha)$ at different temperatures and excess gas quantities that include: (a) 77 K with no excess gas, (b) 177 K with 5×10^{-4} mol of excess gas, and (c) 177 K with 5×10^{-3} mol of excess gas. The contour values for σ^{θ} are in MPa and all plots assume the system is stress-free at the polymer T_g in the absence of gas. The calculations were based on a container with dimensions $R=2\times10^{-2}$ m and $t=2\times10^{-4}$ m and the materials considered were assumed to have a constant $\nu=0.33$ and $T_g=218$ K. Further, the media were assumed to have thermoelastic properties such that $\beta=1$.

from less than 1 MPa to greater than 100 MPa over a realistic range of potential thermoelastic parameters. However, at higher temperatures with excess gas present, the effect of $\Delta\alpha$ on the σ^{θ} diminishes, such that it is almost entirely dependent on E. This is demonstrated in Fig. 3b, which graphically illustrates $\sigma^{\theta}(E,\Delta\alpha)$ at 177 K with 5×10^{-4} mol of excess gas present. It is apparent from the figure that over a significant range of E (two orders of magnitude) the σ^{θ} is essentially independent of thermal expansion mismatch. As more excess gas is added (Fig. 3c), the thermal expansion mismatch plays even less of a role on σ^{θ}.

It is crucial when selecting a material for cryogenic storage that the accumulated stresses remain below the fracture strength of the material under all anticipated conditions. This can be illustrated using the plots in Fig. 3. For example, assume the blood bag material has a fracture strength equal to 50 MPa. Further, assume that during use the blood bag will be cooled to 77 K in the absence of gas, and upon warming to 177 K, 5×10^{-4} mol of excess gas are released. Thus, the material must have corresponding values of E and $\Delta\alpha$ such that they lie to the left of the 50 MPa contour in both Fig. 3a and b. This will ensure that under both conditions where the largest possible stresses can accumulate, the stresses will never exceed the fracture strength and, therefore, failure will not occur. In general, to ensure blood bag integrity, it is imperative that the thermoelastic properties of the material are in regimes that, under anticipated storage conditions, yield tangential stresses well below the fracture strength of the material.

3.3. Blood bag geometry

Another application of the model presented here is to estimate the effects of blood bag geometry on the stress state. The geometry, specifically the local curvature, can play a significant role in the stress state of the material. For example, in regions where the curvature is near zero, the stress due to thermal expansion mismatch or excess gas present will be much lower than the stress in regions of large curvature. Examples of large curvature regions include: weld joints used to seal two polymer sheets together to form the container and kinks and folds that can arise when the bag is filled with medium. Our model incorporates the effect of curvature, R^{-1}, as well as blood bag thickness, t, on the stress state using the concentric sphere geometry described above, where the geometry is completely specified by only two variables, R and t.

From Eq. (13), we see that in the absence of gas, the tangential stress is independent of the blood bag geometry, and therefore, the ratio, R/t. The constant relationship between σ^{θ} and R/t at 77 K in the absence of gas is shown as a solid line in Fig. 4. Note that the independence of geometry is an artifact of the assumption, $R\gg t$, and should no longer be true as R/t approaches zero. In fact, in the limit that R/t goes to zero, the tangential stresses should extend towards infinity. However, we estimate that $R\gg t$ should be an adequate approximation when R/t is greater than about 10.

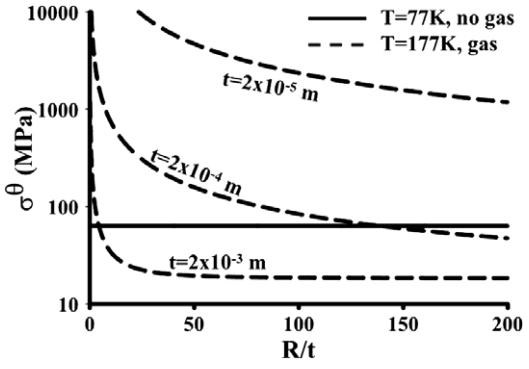

Fig. 4. Effect of blood bag geometry on the tangential stress, σ^{θ}, for two different conditions, $T=77$ K with no excess gas and $T=177$ K with 5×10^{-4} mol of excess gas. Note that in the absence of excess gas the tangential stress is independent of R/t. The plot also shows $\sigma^{\theta}(R/t)$ for the case where excess gas is present for three different values of the container thickness. Values shown in the plots assume that the system is stress-free at the polymer T_g in the absence of gas. The calculations were based on a hypothetical material with $E=10$ GPa, $\nu=0.33$, $\Delta\alpha=3\times10^{-5}$ K^{-1}, and $T_g=218$ K. Further, the media were assumed to have thermoelastic properties such that $\beta=1$.

With the addition of excess gas to the system, our model predicts that the tangential stress is no longer independent of geometry. This is also illustrated in Fig. 4, where the dashed lines indicate $\sigma^{\theta}(R/t)$ for three different values of bag thickness at 177 K with 5×10^{-4} mol of excess gas. For the largest thickness examined, $t=2\times10^{-3}$ m, the model predicts that the tangential stress will be essentially independent of geometry for R/t values greater than approximately 20, and therefore, for R values greater than 0.04 m. Fig. 4 also demonstrates that in the presence of excess gas, as the thickness of the bag decreases, the tangential stress at a given R/t increases. Further, decreasing the thickness of the bag also increases the dependence of the stress on R/t. Thus, it is apparent that the bag geometry can have a significant impact on the magnitude of stress, and therefore the propensity for bag failure.

Just as selection of a material with appropriate thermoelastic properties is critical to avoiding accumulation of stress and fracture, so is the bag design [7]. Large curvature geometric features, such as weld joints or folds induced during use, can result in significant stress accumulation. For example, assume the fracture strength is slightly greater than the geometrically independent stress induced at 77 K in the absence of gas (~63 MPa). If the fracture strength were lower than this value, the bag would always fail under these conditions. However, the dependence of stress on geometry under higher temperature conditions in the presence of excess gas is not as straightforward. For example, assume that the bag has a thickness of 2×10^{-4} m. Then from the plot in Fig. 4, we see that at this thickness, the bag will not fail for R/t values of approximately 140 or greater. This corresponds to $R\geqslant0.028$ m, which results in tangential stresses less than the fracture strength of the hypothetical material. However, if the blood bag is designed such that the effective radius in any region of the bag falls below this value, the model predicts that failure should occur.

Increasing the bag thickness can reduce the accumulated stresses below those required for failure. Again using the relationships illustrated in Fig. 4, a bag that consists of regions with an effective radius of curvature of 0.020 m and thickness of 2×10^{-4} m ($R/t=100$) will accumulate tangential stresses that exceed the hypothetical fracture strength (~63 MPa). However, if the thickness of the blood bag were increased to 2×10^{-3} m, then $R/t=10.0$, which results in stresses well below the critical value. Thus, it is imperative to consider both the effective radii in the bag design and the thickness of the material because both of these factors can have a substantial effect on the overall fracture resistance of blood bags at cryogenic temperatures.

4. Discussion

We have derived an analytical model that can be used to estimate the stress state in blood bags used for cryogenic storage as a function of strain mechanism, material properties, and geometric design. In the applications discussed above, we demonstrated that the model can be used as framework to provide guidance in material selection and product design to avoid failure during use. For example, blood bags used to store HSCs have been fabricated from several different materials, including poly(ethylenevinylacetate) (EVA), fluorinated ethylenepropylene (FEP), and poly(vinylchloride) (PVC) [7]. At cryogenic temperatures, FEP is about an order of magnitude less stiff than EVA, i.e., $E_{\mathrm{PTFE}}\approx0.1E_{\mathrm{EVA}}$. Thus, the model would predict substantially less stress accumulation in blood bags manufactured from FEP compared to those fabricated using EVA. In fact, in laboratories responsible for the storage of HSCs, a significant reduction in blood bag failures was observed when FEP blood bags were used in place of those made of EVA (private communication, David-Ocampo V, NIH/CC/DTM). Although material changes can significantly alter the fracture resistance of a blood bag, for some applications, changing the material is not a possibility. However, the accumulation of stresses can also be reduced by control of blood bag geometry.

Most polymeric blood bags used for cryogenic storage are fabricated by welding two polymer sheets together along the perimeter of the bag. Therefore, the geometry of the blood bag can be characterized as having almost no curvature over most of the bag with very large curvatures in the vicinity of the weld joints. Based on our model, we would expect the bags to be essentially stress-free, except at the welds where large stresses will accumulate. Thus, fracture should always occur at or around the weld joints, and, in fact, for all cryogenically induced bag failures that we have observed, the fracture initiated in the vicinity of a weld joint. The weld geometry is therefore critical in determining the propensity for failure in blood bags used in cryogenic storage applications. Further, the model suggests that lower stresses, and therefore fewer failures, will occur by controlling the welding process so that the curvature at the weld joints is reduced.

In addition to high curvature regions in the blood bag, substantial stresses can accumulate around defects that act as stress concentrators. These defects can be inherent in the polymeric material, such as voids, or they can be induced during manufacturing and handling, such as nicks and scratches. Because these defects act as stress concentrators, they effectively reduce the overall fracture strength of the material. The significance of a defect on strength reduction can be estimated from classical fracture theories, such as the one proposed by Griffith [14]. Using the Griffith fracture condition, we can estimate the size of a critical flaw in the bag in terms of the stresses in our model. Assuming that σ^{θ} is the tensile stress applied to the flawed region in the blood bag, the critical flaw size for failure is $c=2\gamma E/[\pi(\sigma^{\theta})^2]$, where γ is the surface energy of the blood bag material. Thus, an isolated defect smaller than size c is relatively inconsequential; however, defects size c or greater will result in failure for a given σ^{θ} induced in the bag. For a typical polymeric material below T_g, $\gamma\approx0.05$ J/m^2

and $E \approx 10$ GPa. Thus, for an applied tangential stress, σ^{θ}, of 10 MPa, we expect a critical flaw size of about 3 μm.

Thus far we have assumed that the thermoelastic properties of the blood bag material are independent of time and temperature. This may not be the case for all glassy phase polymers. In fact, some polymers, such as fluorinated ethylene propylene mentioned above, may have significant ductility at liquid N_2 temperatures. However, as they are cooled, the material will become significantly stiffer and substantial residual stress may still arise. Further, the release of gas was assumed to be instantaneous at the gas vaporization temperature. This process can, in fact, be slow relative to the temperature changes during thawing. Therefore, it may be important to capture these time and temperature dependencies in the model to accurately predict the magnitude of the stresses that accumulate in the blood bag material. Extension of the current model to these situations is relatively straightforward if the following are known: the time and temperature dependence of the thermoelastic properties of the blood bag, the vaporization rate of the solidified gas, and the cooling and thawing temperature profiles. If these are known, one can simply substitute the functional forms into Eq. (13) (i.e., $E = E(t, T)$, $v = v(t, T)$ and $n = n(t)$) and then integrate the equation over time and temperature as dictated by the temperature profiles to determine the accumulation of stresses. In general, however, these time and temperature dependencies are unknown. Mapping these dependencies would provide insight and guidance into not only bag material and design modifications, but also storage procedure alterations that would result in lower bag failure rates. For example, the ramp rates and dwell times during the storage process can be optimized to minimize stress for a particular bag material.

Another assumption that underpins the formulation of the model is that the gas released from the frozen medium behaves ideally. Generally speaking, the ideal gas approximation is valid at low pressures and high temperatures. To elucidate whether the ideal behavior approximation can be extended to gases under pressure at cryogenic temperatures, we used a newly formulated equation of state of nitrogen for temperature from 63.151 to 1000 K and pressures to 2200 MPa [15]. With these relations we evaluated the ratio of pressure to density (P/ρ) versus temperature (T) for the temperature range 170 K to 230 K (i.e., the temperature, at which the gas evolves, to the potential T_g of the polymer) of nitrogen gas under pressures up to 2.0 MPa (corresponding to $\sigma^{\theta} \sim 100$ MPa). For ideal nitrogen gas, the relationship between P/ρ and T is linear with a slope of 8.314 510 J/(mol K), the molar gas constant. We find that even at $P = 2.0$ MPa the relationship between P/ρ and T over the designated temperature range remains approximately linear (correlation coefficient = 0.968) with a slope of 7.966 ± 0.039, a difference of only -4.2%. At atmospheric pressure ($P = 0.101\ 325$ MPa) the difference is -0.2%. Thus, we conclude that the approximation of ideal gas behavior is adequate under the environmental conditions relevant to this application.

Although the model derived in this manuscript was implemented by making some simplifying assumptions, it provides significant insight into stress accumulation that can lead to failure of blood bags when used to store HSCs under cryogenic conditions. More sophisticated techniques, such as finite element methods, can be employed to determine the stress state with more quantitative accuracy by incorporating the actual bag geometry. However, these more sophisticated methods require detailed, quantitative measurements of the geometry, which are difficult and time consuming to obtain. Thus, the ability to commonly apply these methods to determine stress accumulation is quite limited. However, using our model equations, predictions of the influence of modifications to bag material or bag design on the stress state in the bag can be made easily. Thus, the model equations can be used as guidance in both the manufacture and the usage of blood bags in cryogenic storage applications to limit the accumulation of stresses and, therefore, failure rate of these devices.

5. Summary

We have derived an analytical model for the stress state in blood bags filled with HSCs at cryogenic temperatures based on two potential strain mechanisms: (1) thermal expansion mismatch between the blood bag container and the stored medium (HSCs) and (2) excess gas evolving from the stored medium. The model yields explicit relationships between the stress that accumulates in the container and the thermoelastic properties of the container material, container geometry, and environmental conditions (i.e., temperature and amount of excess gas released from the medium). Based on the model, we have established a quantitative framework to distinguish the relative effects of the two strain mechanisms and the environmental conditions where the maximum accumulated stresses occur. Further, we have used the model to elucidate the influence of the thermoelastic properties of the bag material on the accumulation of stresses. Our findings suggest that the magnitude of accumulated stress will be substantially lower in softer materials (low E) and those that have thermal expansion coefficients similar to the medium (low $\Delta\alpha$). This is consistent with the observed reduction in failures witnessed when containers comprised of softer materials were used in laboratories responsible for the storage of HSCs. Thus, materials selection is a critical aspect of the product design. We have also used the model to explore the effect of container geometry on the accumulated stresses. We find that the largest stresses will accumulate in thin, high curvature regions of the container. This finding is consistent with observations that suggest that most, if not all, bag failures initiate in the vicinity of weld joints in the containers. Thus, the geometric design of the product is also critical to preventing future container failures. Finally, although many simplifying assumptions were made in the derivation of the model, the equations provide much insight into the strain mechanisms, as well as blood bag material and design

considerations, which impact the accumulation of stresses that lead to bag failure during cryogenic storage of HSCs. These equations can be used as guidance for bag material selection and bag design to limit the accumulation of stresses and, therefore, failure rate of these devices.

Disclaimer

Statements in this manuscript reflect the opinions of the authors and do not necessarily reflect the opinions of the US Food and Drug Administration. The mention of commercial products, their source, or their use in connection with the material reported herein is not to be construed as either an actual or implied endorsement by either the US Food and Drug Administration or the National Institute of Standards and Technology.

Acknowledgements

The authors would like to thank Ellen F. Lazarus, M.D. (FDA), Herb Cullis (American Fluoroseal Corporation) and Virginia David-Ocampo (NIH) for their helpful advice and criticisms. Furthermore, the authors would like to thank Brian Lawn (NIST), Sheldon Wiederhorn (NIST), and Grady White (NIST) for their suggestions and critical review of this manuscript.

Appendix A

By symmetry the displacements for the models shown schematically in Fig. 1 are everywhere radial. In this case a general expression for the radial displacement is given by [16]

$$U = -h \cdot r - \frac{g}{2 \cdot r^2}, \tag{A.1}$$

where r is the radial coordinate, and h and g are constants to be determined by the boundary conditions. The strains are given by [15]

$$\varepsilon^r = \frac{\partial U}{\partial r} = -h + \frac{g}{r^3}, \tag{A.2a}$$

$$\varepsilon^\theta = \varepsilon^\phi = \frac{U}{r} = -h - \frac{g}{2 \cdot r^3}, \tag{A.2b}$$

$$\varepsilon^{r\theta} = \varepsilon^{r\phi} = \varepsilon^{\theta\phi} = 0. \tag{A.2c}$$

The elastic strain is the total strain, Eqs. (A.2), minus the thermal strain, $\alpha_{ij}\Delta T$, where α_{ij} is the coefficient of thermal expansion tensor and ΔT is the temperature change from the stress-free state. Accordingly, the stresses are given by

$$\sigma^r = \frac{E}{(1+v)(1-2v)}[(1-v)\varepsilon^r + 2v\varepsilon^\theta - (1+v)\alpha\Delta T] = -H + \frac{G}{r^3}, \tag{A.3a}$$

$$\sigma^\theta = \sigma^\phi = \frac{E}{(1+v)(1-2v)}[\varepsilon^\theta + v\varepsilon^r - (1+v)\alpha\Delta T] = -H - \frac{G}{2 \cdot r^3}, \tag{A.3b}$$

$$\sigma^{r\theta} = \sigma^{r\phi} = \sigma^{\theta\phi} = 0, \tag{A.3c}$$

where E is the Young's modulus, v is the Poisson's ratio, and α is the coefficient of thermal expansion. The new constants H and G are related to h and g, respectively, as

$$H = \frac{E \cdot (h + \alpha\Delta T)}{(1-2v)}, \tag{A.4a}$$

$$G = \frac{Eg}{(1+v)}, \tag{A.4b}$$

For a frozen biological medium of radius a and external pressure P, $G_1 = 0$, since the stress and strain are finite at the origin ($r = 0$), and $H_1 = P$. Accordingly, the stress state is hydrostatic and uniform:

$$\sigma_1^r = \sigma_1^\theta = \sigma_1^\phi = -P, \tag{A.5}$$

The strains and displacement are given by

$$\varepsilon_1^r = \varepsilon_1^\theta = \varepsilon_1^\phi = \frac{U_1(r)}{r} = -\frac{P(1-2v_1)}{E_1} + \alpha_1\Delta T, \tag{A.6}$$

For the polymeric container of inner radius a and outer radius b, internal pressure P, and atmospheric outer pressure (≈ 0), $H_2 = G_2/b^3 = -Pa^3/(b^3 - a^3)$. Accordingly, the stresses are given by

$$\sigma_2^r = -P\left(\frac{a}{r}\right)^3\left(\frac{b^3 - r^3}{b^3 - a^3}\right), \tag{A.7a}$$

$$\sigma_2^\theta = \sigma_2^\phi = \frac{1}{2}P\left(\frac{a}{r}\right)^3\left(\frac{b^3 + 2r^3}{b^3 - a^3}\right), \tag{A.7b}$$

The strains and the radial displacement are given by

$$\varepsilon_2^r = -\frac{P}{E_2}\left(\frac{a}{r}\right)^3\left[\frac{(1+v_2)b^3 - (1-2v_2)r^3}{b^3 - a^3}\right] + \alpha_2\Delta T, \tag{A.8a}$$

$$\varepsilon_2^\theta = \varepsilon_2^\phi = \frac{U_2(r)}{r} = \frac{1}{2}\frac{P}{E_2}\left(\frac{a}{r}\right)^3\left[\frac{(1+v_2)b^3 + 2(1-2v_2)r^3}{b^3 - a^3}\right] + \alpha_2\Delta T, \tag{A.8b}$$

For a thin-wall container of radius $R = b$ and thickness $t = (b - a) \ll R$, Eqs. (7) and (8) can be approximated, respectively, by

$$\sigma_2^r = -\left(\frac{\rho}{t}\right)P, \tag{A.9a}$$

$$\sigma_2^\theta = \sigma_2^\phi = \left(\frac{R}{2t}\right)P, \tag{A.9b}$$

and

$$\varepsilon_2^r = -\frac{2v_2P}{E_2}\left(\frac{R}{2t}\right) + \alpha_2\Delta T, \tag{A.10a}$$

$$\varepsilon_2^\theta = \varepsilon_2^\phi = \frac{U_2(r)}{R} = \frac{(1-v_2)P}{E_2}\left(\frac{R}{2t}\right) + \alpha_2\Delta T, \tag{A.10b}$$

where $\rho = (R - r) \ll R$ and $t \ll R$.

References

[1] Horowitz MM. Uses and growth of hematopoietic cell transplantation. In: Thomas ED, Blume KG, Foreman SJ, editors. Hematopoietic cell transplantation. Malden, MA: Blackwell Science; 1999. p. 12–8.

[2] International Standards Organization (ISO). ISO 3826-1 Plastics collapsible containers for human blood and blood components, Part 1: Conventional containers. Geneva: International Organization for Standardization; 2003.
[3] Stiff PJ. Cryopreservation of hematopoietic stem cells. In: Foreman SJ, Blume KG, Thomas ED, editors. Bone marrow transplantation. Boston, MA: Blackwell Scientific; 1994. p. 299–308.
[4] Hmel PJ, Kennedy A, Quiles JG, Gorogias M, Seelbaugh JP, Morrissette CR, et al. Physical and thermal properties of blood storage bags: implications for shipping frozen components on dry ice. Transfusion 2002;42:836–46.
[5] Khuu HM, Cowley H, David-Ocampo V, Carter CS, Kasten-Sportes C, Wayne AS, et al. Catastrophic failures of freezing bags for cellular therapy products: description, cause, and consequences. Cytotherapy 2002;4:539–49.
[6] Ward IM, Hadley DW. An introduction to the mechanical properties of solid polymers. Indianapolis, IN: John Wiley and Sons; 1993, p. 268–99.
[7] Shang SW, Ling MTK, Westphal SP, Woo L. Correlate resin properties to the cryogenic impact performance of medical containers. ANTEC: Conf Proc 1996;3:2862–5.
[8] Yamaoka H, Miyatra K, Yano O. Cryogenic properties of engineering plastic films. Cryogenics 1995;35:787–9.
[9] Hartwig G. Polymer properties at room and cryogenic temperatures. New York, NY: Plenum Press; 1994.
[10] Hartwig G. Cryogenic properties. In: Mark HF, Kroschwitz JI, editors. Encyclopedia of polymer science and engineering, vol. 4. New York, NY: John Wiley and Sons; 1985. p. 450–82.
[11] Yano O, Yamaoka H. Cryogenic properties of polymers. Prog Polym Sci 1995;20:585–613.
[12] Rottger K, Endriss A, Ihringer J. Lattice constants and thermal expansion of H_2O and D_2O ice in between 10 and 265 K. Acta Crystallogr B 1994;50:644–8.
[13] Hsueh CH, Fuller Jr ER. Analytical modeling of oxide thickness effects on residual stresses in thermal barrier coatings. Scripta Mater 2000;42:781–7.
[14] Courtney TH. In: Clark BJ, Morriss JM, editors. Mechanical behavior of materials. New York, NY: McGraw-Hill; 1990. p. 405–7.
[15] Span R, Lemmon EW, Jacobsen RT, Wagner W, Yokozeki A. A reference equation of state for the thermodynamic properties of nitrogen for temperatures from 63.151 to 1000 K and pressures to 2200 MPa. J Phys Chem Ref Data 2000;29: 1361–433.
[16] Love AEH. A treatise on the mathematical theory of elasticity. Article 98. 4th ed. New York, NY: Dover; 1927.